

University of Groningen

## Diffusive motion of antiphase domain boundaries in Fe<sub>3</sub>O<sub>4</sub> films

Eerenstein, W; Palstra, TTM; Hibma, T; Celotto, S

*Published in:*  
Physical Review. B: Condensed Matter and Materials Physics

*DOI:*  
[10.1103/PhysRevB.68.014428](https://doi.org/10.1103/PhysRevB.68.014428)

**IMPORTANT NOTE:** You are advised to consult the publisher's version (publisher's PDF) if you wish to cite from it. Please check the document version below.

*Document Version*  
Publisher's PDF, also known as Version of record

*Publication date:*  
2003

[Link to publication in University of Groningen/UMCG research database](#)

### *Citation for published version (APA):*

Eerenstein, W., Palstra, TTM., Hibma, T., & Celotto, S. (2003). Diffusive motion of antiphase domain boundaries in Fe<sub>3</sub>O<sub>4</sub> films. *Physical Review. B: Condensed Matter and Materials Physics*, 68(1), art - 014428. [014428]. <https://doi.org/10.1103/PhysRevB.68.014428>

### **Copyright**

Other than for strictly personal use, it is not permitted to download or to forward/distribute the text or part of it without the consent of the author(s) and/or copyright holder(s), unless the work is under an open content license (like Creative Commons).

The publication may also be distributed here under the terms of Article 25fa of the Dutch Copyright Act, indicated by the "Taverne" license. More information can be found on the University of Groningen website: <https://www.rug.nl/library/open-access/self-archiving-pure/taverne-amendment>.

### **Take-down policy**

If you believe that this document breaches copyright please contact us providing details, and we will remove access to the work immediately and investigate your claim.

*Downloaded from the University of Groningen/UMCG research database (Pure): <http://www.rug.nl/research/portal>. For technical reasons the number of authors shown on this cover page is limited to 10 maximum.*

# Diffusive motion of antiphase domain boundaries in $\text{Fe}_3\text{O}_4$ films

W. Eerenstein,\* T. T. M. Palstra, and T. Hibma

*Material Science Center, University of Groningen, Nijenborgh 4, 9747 AG Groningen, The Netherlands*

S. Celotto

*Department of Engineering, Materials Science and Engineering, University of Liverpool, Brownlow Hill, Liverpool L69 3BX, United Kingdom*

(Received 26 February 2003; published 25 July 2003)

The antiphase domain structure in epitaxial  $\text{Fe}_3\text{O}_4$  films determines its physical properties such as superparamagnetism, resistivity, and magnetoresistance. A good knowledge and control of the domain sizes in these films is therefore of utmost importance. We report on the finding that the antiphase domain boundaries anneal out via a diffusive mechanism at relatively low temperatures. This has been demonstrated by postannealing the films at 250 °C, 300 °C and 350 °C. The boundary migration process is a thermally activated process with an activation energy of 26 kJ/mol (250 meV). We have further studied the domain size in epitaxial  $\text{Fe}_3\text{O}_4$  films as a function of growth parameters. A linear relationship has been obtained for the logarithm of the domain size versus the inverse of the growth temperature (in the range of 125 °C to 300 °C), which supports the diffusional mechanism. The domain size is not influenced by the iron flux, but does depend on the oxygen flux. This suggests that the critical nuclei are pairs of iron and oxygen atoms and that iron is more mobile than oxygen.

DOI: 10.1103/PhysRevB.68.014428

PACS number(s): 68.35.Fx, 68.55.Ac, 68.55.Jk, 68.37.Lp

## I. INTRODUCTION

Epitaxial  $\text{Fe}_3\text{O}_4$  films grown on MgO substrates are known to contain antiphase domain boundaries (APBs).<sup>1–3</sup> The APBs are natural growth defects, resulting from the fact that the lattice constant of  $\text{Fe}_3\text{O}_4$  ( $a=8.3987$  Å) is twice as large as the one of MgO ( $a=4.212$  Å). In a previous publication it was assumed that the APBs are formed in the first monolayer, with fixed domain size as subsequent layers are deposited.<sup>2</sup> In this paper, we show this to be incorrect and that instead the APBs are mobile and anneal out by a diffusive mechanism.

The presence of the APBs influences the magnetic and electronic properties of the films. For example, the magnetization does not saturate in high fields<sup>1</sup> and ultrathin films below 5 nm show superparamagnetic behavior.<sup>2</sup> A large fraction of the APBs exhibits a strong antiferromagnetic (AF) coupling.<sup>1,2</sup> Here the conduction electrons that have a high degree of spin polarization<sup>8</sup> are blocked. The resistivity of epitaxial  $\text{Fe}_3\text{O}_4$  films containing APBs is thus increased with respect to the bulk resistivity. The resistivity of the films also increases with decreasing film thickness. Recently we have shown<sup>4</sup> that this can be related to a significant decrease in domain size, and thus to a strong increase in APB density. Upon application of a magnetic field, the AF spins change their orientation with respect to each other and the resistivity is reduced. The magnetoresistance behavior for one boundary has been modeled by a hopping model in which spin-polarized electrons traverse an antiferromagnetic interface between two ferromagnetic chains.<sup>5–7</sup> The magnetoresistance effect across one boundary is expected to be very large. However, in the  $\text{Fe}_3\text{O}_4$  films the domain size is very small (<50 nm) and the magnetoresistance (MR) is thus measured over many boundaries. This greatly reduces the MR effect and complicates the modeling of the MR behavior in  $\text{Fe}_3\text{O}_4$

films. Therefore, a large domain size is desirable in order to measure the magnetoresistance of a single boundary.

Since the domain boundaries determine general physical properties such as magnetism and resistivity, it is necessary to have knowledge about the boundary density. For instance, the saturation magnetization of  $\text{Fe}_3\text{O}_4$  films grown by different techniques and temperatures [i.e., sputtering<sup>1</sup> and molecular-beam epitaxy<sup>2,3</sup> (MBE)] is very different and could be related to a different APB structure.<sup>9</sup> In this paper we present a quantitative study of the changes in APB density as a function of annealing and growth parameters.

## II. EXPERIMENT

The  $\text{Fe}_3\text{O}_4$  films were grown using MBE in an ultrahigh vacuum system with a background pressure of  $10^{-10}$  mbar. Standard samples were grown using an iron flux of 1.2 Å/min, an oxygen background pressure of  $10^{-6}$  mbar, and a growth temperature of 250 °C. Using these conditions, films between 3 and 100 nm thickness were grown. To determine the structural quality and purity, the films were analyzed *in situ* using reflection high-energy electron diffraction (RHEED), low-energy electron diffraction and x-ray photoemission spectroscopy. The thickness of the films was determined both during growth from the oscillation period of the RHEED specular spot intensity and after growth from x-ray reflectivity.

The iron flux was measured using a quartz-crystal balance. Oxygen was admitted via a gas delivery system consisting of a small buffer volume. The  $\text{O}_2$  gas is let into the buffer volume via a leak valve. The buffer pressure is measured with a baratron.

The domain sizes have been studied by transmission electron microscopy (TEM). Specimens were prepared by dissolving the MgO substrate and floating the  $\text{Fe}_3\text{O}_4$  films off in

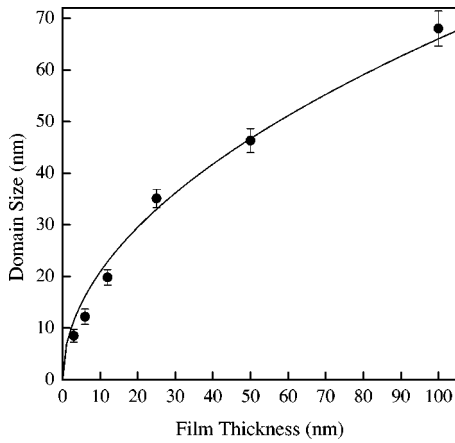


FIG. 1. Domain sizes for 3, 6, 12, 25, 50, and 100 nm thick epitaxial  $\text{Fe}_3\text{O}_4$  films on MgO. The domain size is determined from dark field TEM images obtained with a (220) spinel reflection. The line is a fit to the data  $D = C\sqrt{t}$ .

a 4-wt % ammonium sulfate  $[(\text{NH}_4)_2\text{SO}_4]$  solution at  $70^\circ\text{C}$ .<sup>10</sup> The  $\text{Fe}_3\text{O}_4$  films were picked up on a copper grid and analyzed in a JEOL 2000FX electron microscope operating at 200 keV. To analyze the domain size, dark field images were made using a (220)-type spinel reflection. In the  $\text{Fe}_3\text{O}_4$  films, seven types of boundary shifts are possible:  $1/4[011]$ ,  $1/4[01\bar{1}]$ ,  $1/4[101]$ ,  $1/4[10\bar{1}]$ ,  $1/4[110]$ ,  $1/4[1\bar{1}0]$ , and  $1/2[100]$ , of which only the first four are visible when using a (220)-type reflection. All the domain sizes reported here refer to the domain size as obtained from the dark field (220) images taken with this type of reflection. Quantitative domain sizes have been determined from the dark field images using the linear intercept method.

### III. RESULTS AND DISCUSSION

The formation of APBs in epitaxial  $\text{Fe}_3\text{O}_4$  films results from the nucleation of islands when the films are deposited on the substrate. Previous studies have assumed that the APBs form in the first monolayer and the domain size is then fixed as the APBs continue to extend upwards through the film as more material is deposited.<sup>2</sup>

We recently reported that the domain size depends on the thickness of the film. The domain size increases significantly with film thickness, and therefore with deposition time, according to the parabolic relation  $D \propto \sqrt{t}$  as shown in Fig. 1.

The increase in domain size with thickness can originate from two effects. One possibility is that small domains are formed in the first monolayer and larger domains grow on top of these as the film thickness increases. The other possibility is that the APBs migrate laterally during the growth process such that the domain size increases.

To discriminate between these two options, we have studied the development of the domain sizes for 12-nm thick films by postannealing them at  $250^\circ\text{C}$ ,  $300^\circ\text{C}$ , and  $350^\circ\text{C}$  for 1, 2, 4, and 10 hours. Figure 2 shows TEM images of the 12-nm thick reference sample [Fig. 2(a)] and of samples that were postannealed for 1 and 2 h at  $300^\circ\text{C}$  [Figs. 2(b) and 2(c), respectively]. The postannealing was performed in an

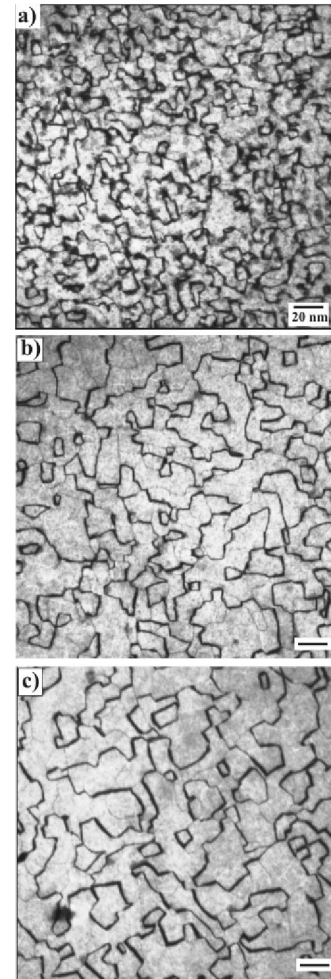


FIG. 2. Dark field TEM images of 12-nm thick  $\text{Fe}_3\text{O}_4$  films. The as-grown film is shown in (a) and the images in (b) and (c) were taken after postannealing at  $300^\circ\text{C}$  in an oxygen background pressure of  $10^{-6}$  mbar for 1 and 2 h, respectively. The scale bar is in all cases 20 nm. Images were taken with a (220)-type reflection near the  $[001]$  zone axis.

oxygen background pressure of  $10^{-6}$  mbar, which is the same as that which took place during the growth of the films. It is clear that the domain size increases with annealing time. These measurements therefore support the interpretation that the APBs anneal out during the growth of the films. This is confirmed by the TEM images (see Fig. 2). If larger domains were to form on top of smaller ones, the small domains would still be visible in the TEM images, which is not the case. The growth of the antiphase domains in epitaxial  $\text{Fe}_3\text{O}_4$  films is surprising, as one would expect the APBs to be static. Antiphase domain growth has been observed in  $\text{Mg}_2\text{TiO}_4$  films,<sup>11</sup> but these films were grown with the solid-state reaction technique which requires diffusion of one species into the other and high temperatures (about  $1000^\circ\text{C}$ ).

The measured domain sizes for the as-grown and the postannealed samples at the three different temperatures are shown in Fig. 3. The rate law for domain coarsening can generally be described as<sup>12,14</sup>

$$D^n - D_0^n = kt_a, \quad (1)$$

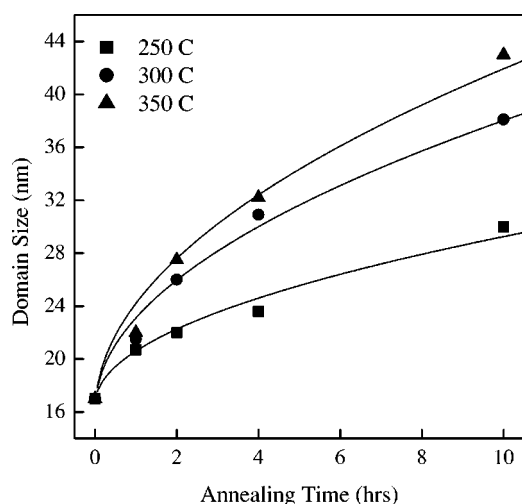


FIG. 3. Increase in domain size for 12-nm thick Fe<sub>3</sub>O<sub>4</sub> films with annealing times 1, 2, 4, and 10 h. Annealing has been done at 250 °C, 300 °C, and 350 °C. Lines are guides to the eye.

with  $k$  being the rate constant,  $D_0$  the domain size at the start of annealing, and  $t_a$  the annealing time. When  $n=2$ ,  $k$  has the same dimensions as a diffusion coefficient (m<sup>2</sup>/s). This rate law results from the driving force for migration being the APB surface energy and the curvature of the APBs.<sup>25</sup> If the boundary migration mechanism is a thermally activated process, the rate constant  $k$  has the form  $k = k_0 e^{-E_a/k_B T}$ .

The antiphase domain coarsening in our Fe<sub>3</sub>O<sub>4</sub> films is well described by Eq. (1) with  $n=2$ , as shown in Figs. 4(a)–4(c) where the plot of  $D^2 - D_0^2$  versus the annealing time yields a straight line. The slopes of the graphs give values of  $k$  at three different temperatures. The logarithm of  $k$  versus  $1/T$  [Fig. 4(d)] gives an activation energy of  $26 \pm 5$  kJ/mol.

APB migration following the same rate law as that in Eq. (1) and with  $n=2$  has also been found in other materials. For instance, in Cu<sub>3</sub>Au in which the activation energy is 184 kJ/mol (Ref. 13) and in anorthite (CaAl<sub>2</sub>Si<sub>2</sub>O<sub>8</sub>) the activation energy is 514 kJ/mol.<sup>14</sup> In both cases, the activation energy for boundary migration is comparable to values obtained using bulk tracer and interdiffusion experiments.<sup>13,14</sup>

Compared to the above-mentioned materials, the activation energy for domain coarsening in Fe<sub>3</sub>O<sub>4</sub> films is relatively low. APB migration in ordered metallic systems such as Cu<sub>3</sub>Au requires substitutional diffusion and hence activation values are similar to bulk diffusion for these materials. However, for Fe<sub>3</sub>O<sub>4</sub> the oxygen sublattice is continuous across the boundary and APB migration only requires diffusion of the cation species on the mostly unoccupied interstitial sites of the oxygen sublattice. Consequently, the activation energy for interstitial cation diffusion would be expected to be significantly less than that for substitutional diffusion of ordered metallic systems. Anorthite also has an fcc oxygen sublattice which is continuous across the boundary. The difference in activation energy for domain coarsening between Fe<sub>3</sub>O<sub>4</sub> and anorthite is about an order of magnitude. The APB coarsening in anorthite requires an exchange of Al and Si,<sup>14</sup> whereas in Fe<sub>3</sub>O<sub>4</sub> a translation of the iron ions is involved. Carpenter has shown<sup>15</sup> that APBs that require only

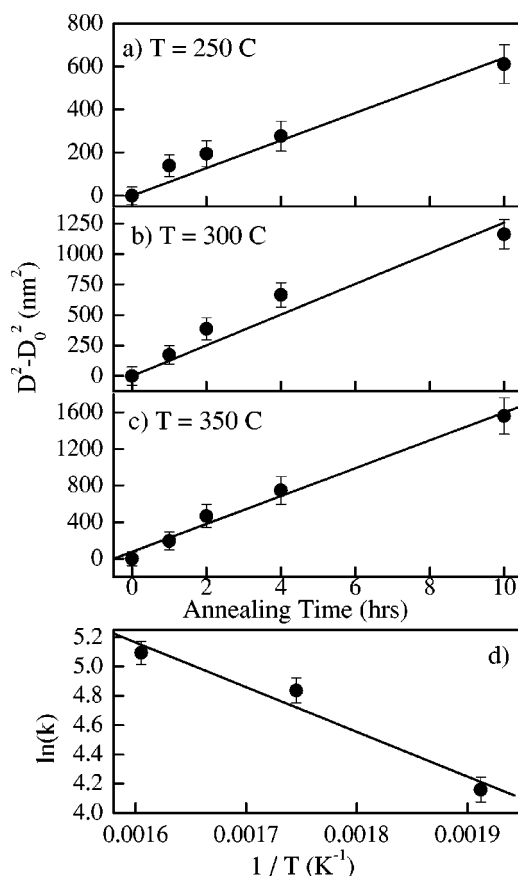


FIG. 4. Square of the domain size versus annealing time at (a) 250 °C, (b) 300 °C, and (c) 350 °C. The slopes of these three curves are shown in (d).

a small atomic displacement migrate much faster than APBs that require an exchange of cations. Furthermore, the two materials have different electronic properties. Anorthite is nonconducting and point defects will build up electrostatic interaction, inhibiting the motion of the cations, especially at high defect concentrations. Fe<sub>3</sub>O<sub>4</sub>, on the other hand, has a rapid exchange of electrons between Fe<sup>2+</sup> and Fe<sup>3+</sup> and no long-range electrostatic interactions can build up.<sup>16</sup>

It is also interesting to compare our activation energy to bulk diffusion data. A comprehensive study of the bulk diffusion in Fe<sub>3</sub>O<sub>4</sub> has been performed by Dieckmann and Schmalzried.<sup>17–19</sup> They performed tracer diffusion experiments as a function of temperature and oxygen pressure. The main result was that diffusion occurred via a defect mechanism and was therefore strongly dependent on the oxygen pressure ( $pO_2$ ), because the formation of point defects depends on  $pO_2$ . At low  $pO_2$  the bulk diffusion mechanism was dominated by iron interstitials. Diffusion via interstitial sites is complicated and several mechanisms have been proposed.<sup>20,21</sup> At high  $pO_2$  diffusion occurs mainly via vacancies on the octahedral iron lattice, which has also been confirmed by Mössbauer studies.<sup>22</sup> The migration enthalpy for vacancy diffusion is 86.5 kJ/mol and for interstitial diffusion it is 255.6 kJ/mol.<sup>23</sup> Even though the bulk values have been obtained from experiments that have been performed at temperatures far above the Curie temperature ( $T_c$ ), Atkinson



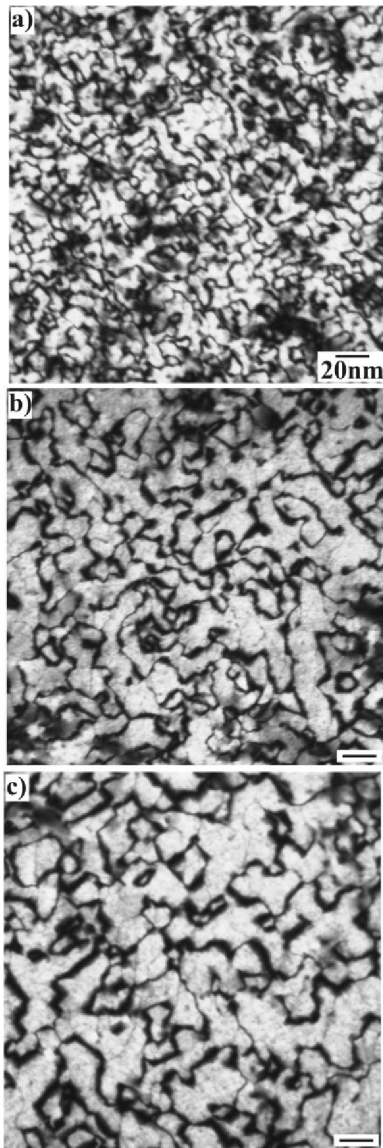


FIG. 5. Dark field TEM images of 12-nm thick  $\text{Fe}_3\text{O}_4$  films. The as-grown film is shown in (a) and the images in (b) and (c) were taken after postannealing at 300 °C in vacuum for 1 and 2 h, respectively. The scale bar is in all cases 20 nm.

*et al.* have performed tracer diffusion experiments below  $T_c$  and found that the high-temperature data can be extrapolated to temperatures below  $T_c$ .<sup>24</sup> The activation energy for bulk diffusion is higher than for domain coarsening. A possible explanation is that bulk diffusion requires the formation of point defects, while in epitaxial films, a defect structure on the Fe sublattice is already present at the APBs, which could facilitate migration along the APBs. We have also postannealed a 12-nm thick  $\text{Fe}_3\text{O}_4$  film at 300 °C in vacuum. Images of the as-grown sample and after postannealing for 1 and 2 h are shown in Fig. 5.

While the boundaries are sharper for the samples that have been postannealed in oxygen, the domain sizes are to within 10% equal for annealing in vacuum and in oxygen. The fact that the migration of the APBs is independent of the presence of oxygen during annealing indicates that boundary

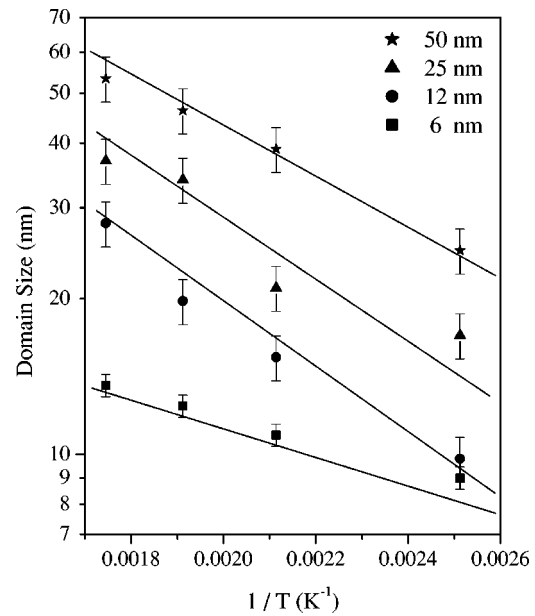


FIG. 6. Domain sizes versus growth temperature for 6 nm, 12 nm, 25 nm, and 50 nm thick films.

migration does not require additional defects to be formed, since a defect structure already exists at the APBs.

Due to the high density of APBs the free energy of the thin films is much higher than for an APB-free single crystal. The epitaxial films thus possess a large driving force for APB removal. The situation can be compared to a polycrystalline film with grain boundaries. Due to the larger free energy of this system compared to a single crystal the film is not stable. Annealing these films causes the boundaries to migrate, such that a local equilibrium at the boundaries can be achieved. Equilibrium at a boundary junction depends on the surface energy of the boundaries, the number of boundaries intersecting at a junction, the angle between the boundaries, and the curvature of the boundaries.<sup>25</sup> Small grains tend to have high curvature boundaries and these grains disappear during annealing. A similar situation occurs in the epitaxial  $\text{Fe}_3\text{O}_4$  films. The as-grown film has a large number of junctions where three or more boundaries meet [Figs. 2(a) and 5(a)]. Furthermore, the APB directionality is random with a curved APB structure. After annealing, the boundaries have become straighter and the number of junctions is significantly reduced [Figs. 2(b), 2(c), 5(b), 5(c)].

If the mechanism for domain coarsening during growth is a diffusional process, a change in domain size can be expected for different growth temperatures [because the rate constant  $k$  in Eq. (1) depends on temperature as  $k = k_0 e^{-E_a/k_B T}$ ]. To investigate this aspect,  $\text{Fe}_3\text{O}_4$  films of 6, 12, 25, and 50 nm thickness were prepared at 125 °C, 200 °C, and 300 °C, keeping the iron and oxygen fluxes constant. For higher temperatures, Mg from the substrate starts to segregate into the film,<sup>26</sup> thus limiting the maximum growth temperature.

The domain sizes for various film thicknesses (6, 12, 25, and 50 nm) versus  $1/T$  are shown in Fig. 6. On a logarithmic scale, this is indeed a straight line. The activation energies are 22, 19, and 17 kJ/mol for 12, 25, and 50 nm, respectively.

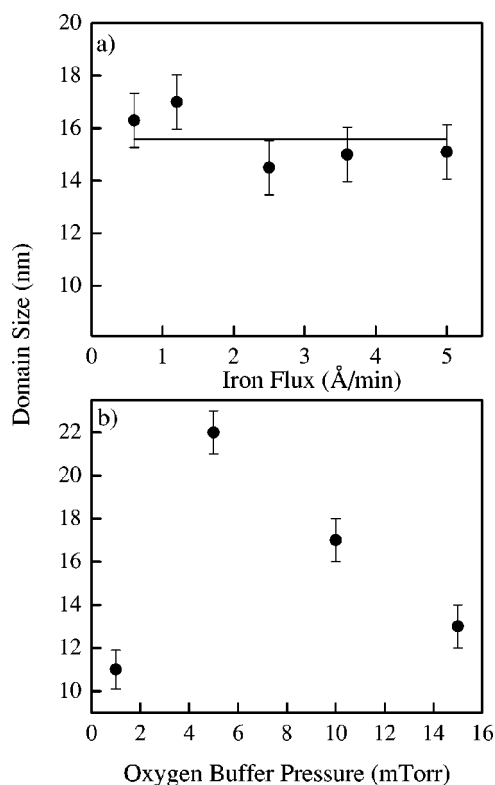


FIG. 7. Domain sizes for 12-nm thick  $\text{Fe}_3\text{O}_4$  films grown at  $250^\circ\text{C}$  as a function of (a) iron flux and (b) oxygen flux.

Within experimental uncertainty these values are the same as the one obtained for postannealing. This shows that the same mechanism applies to coarsening during growth. The 6-nm thick film has a much lower activation energy of  $9 \pm 1$  kJ/mol. This is probably due to the extremely high APB density in this film<sup>4</sup> leading to an increased driving force for APBs migration.

The initial domain size formed in the first monolayer can also depend on the oxygen or iron flux. We have studied the influence of the iron flux by growing 12nm thick samples using 0.6, 1.2, 2.5, 3.6, and 5  $\text{\AA}/\text{min}$  iron fluxes, keeping the oxygen buffer pressure constant at 10 mTorr. The domain sizes of 12-nm thick films grown at  $250^\circ\text{C}$  with different iron fluxes are shown in Fig. 7(a). The domain size is within experimental error independent of the iron flux.

In contrast, a clear change in domain size is observed if the oxygen flux is varied [Fig. 7(b)]. The 12-nm thick specimens were grown at a constant iron flux of  $1.2 \text{ \AA}/\text{min}$  [ $1.8 \times 10^{17} (\text{m}^{-2}\text{s}^{-1})$ ] using different oxygen fluxes. The oxygen flux is expressed in terms of the baratron buffer pressure (in mTorr). To obtain the oxygen flux,  $F(\text{O}_2)$ , in particles/ $\text{m}^2\text{s}$ , the following relation holds:  $F(\text{O}_2) = 1.9 \times 10^{17} \times P_{\text{buf}}$ . For oxygen buffer pressures between 5 and 15 mTorr, the domain size decreases with increasing oxygen pressure.

When an oxygen buffer pressure of 1 mTorr is used, the domain size is smallest. At this oxygen pressure, the flux of  $\text{O}_2$  molecules is  $1.9 \times 10^{17} (\text{m}^{-2}\text{s}^{-1})$ . The iron flux is  $1.8 \times 10^{17} (\text{m}^{-2}\text{s}^{-1})$ . The oxygen flux necessary to oxidize the iron into  $\text{Fe}_3\text{O}_4$  is  $2.4 \times 10^{17} (\text{m}^{-2}\text{s}^{-1})$ . Therefore, the  $\text{O}_2$  flux is too low to fully oxidize all the iron into  $\text{Fe}_3\text{O}_4$ .

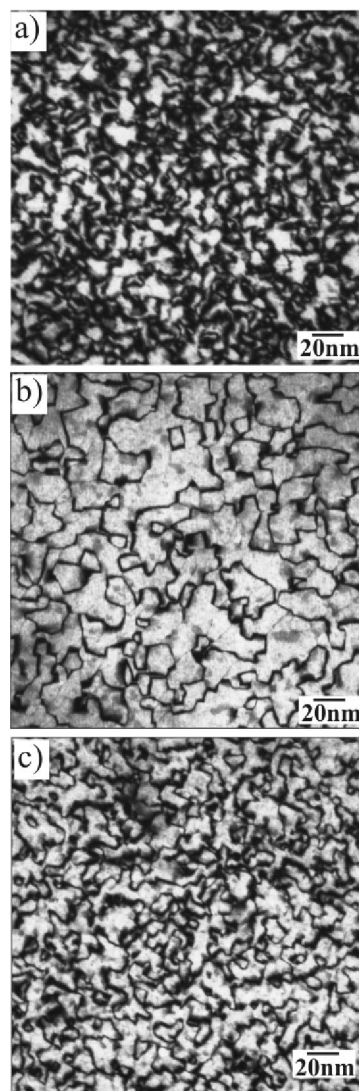


FIG. 8. Dark field TEM images of 12-nm thick  $\text{Fe}_3\text{O}_4$  films grown with a constant iron flux, but with a varying oxygen fluxes of (a) the lowest applied oxygen flux ( $P_{\text{buf}}=1$  mTorr), (b)  $P_{\text{buf}}=5$  mTorr, and (c)  $P_{\text{buf}}=15$  mTorr.

TEM images of the 12-nm thick  $\text{Fe}_3\text{O}_4$  films grown at different oxygen pressures are shown in Fig. 8. The antiphase domain boundaries of the two samples with small domain sizes, Figs. 8(a) and 8(c) appear broader than the APBs of the film with a larger domain size [Fig. 8(b)], for reasons that are unclear.

The fact that the domain size is independent of the iron flux but decreases with increasing oxygen flux is quite surprising at first sight, but can be explained using general nucleation and growth theoretical arguments. We will start the discussion with the simpler case of the nucleation and growth of an elemental metal and follow the treatment of Villain *et al.*<sup>27</sup> Adatoms are deposited at random with a flux  $F$  per unit area and time. It is assumed that the critical nucleus is a dimer and that the detachment of atoms from islands and evaporation can be neglected. During the initial stage of growth, the adatom density rises rapidly, leading to an increase in the island density as the adatoms start to ag-

gregate. At a certain coverage, the average separation between the islands becomes so small that most adatoms are captured by an island instead of forming new nuclei. At this stage, the maximum island density is reached. The average size of the islands is thus determined by the balance between the deposition rate and the surface diffusion constant of the adatoms. An approximate value can be obtained as follows.

In the initial stage of the growth, the adatom has to move a distance  $L$  before being absorbed. In doing so, it visits approximately  $L^2$  sites. The chance to find a site occupied is  $\rho$  (the density of adatoms) and therefore the nucleation rate is

$$\frac{1}{\tau_{nuc}} = FL^2\rho. \quad (2)$$

Another approximate expression for the nucleation rate can be obtained by realizing that during the time necessary to complete one atomic layer one nucleus is formed per  $L^2$  sites,<sup>27,29</sup> i.e.,  $1/\tau_{nuc} = F/L^2$ . Combining the above two equations yields

$$L = (\rho)^{-1/4}. \quad (3)$$

The density of adatoms can be obtained from the product of the flux and the average lifetime,  $\tau$ , of an adatom. The average lifetime is approximately equal to  $L^2/D$ , where  $D$  is the adatom diffusion constant. As a result, the average adatom density can be expressed as

$$\rho = F\tau = \frac{FL^2}{D} \quad (4)$$

and the familiar result<sup>28–30,27</sup>

$$L = \left(\frac{D}{F}\right)^{1/6} \quad (5)$$

is obtained.

We apply similar arguments to the growth of iron oxide, which is obviously a much more complicated system. For the MBE growth of  $\text{Fe}_3\text{O}_4$  the growth mechanism is not known and during deposition there are two fluxes, the iron flux and the oxygen flux.

We assume that a critical nucleus is formed when an Fe adatom and an oxygen particle meet. The precise form of the oxygen species, whether it is molecular or atomic oxygen, is not known. We will assume that the metal particle is diffusing at a much faster rate than the oxygen species. In that case the iron adatom visits  $L^2$  sites before it is captured. The probability that it meets an oxygen particle and forms an oxide nucleus is equal to the average density of oxygen particles  $\rho_O$ . The nucleation rate of oxide particles then becomes

$$\frac{1}{\tau_{nuc}} = F_{Fe}L^2\rho_O. \quad (6)$$

If the growth is limited by the iron flux, one oxide nucleus is formed per  $L^2$  sites during the time  $1/F_{Fe}$  necessary to form

a full monolayer, and consequently the nucleation time is also equal to  $1/\tau_{nuc} = F_{Fe}/L^2$ . Combining the last two equations one finds

$$L = (\rho_O)^{-1/4}. \quad (7)$$

The island size thus depends on the oxygen particle density only. It is independent of the iron flux, in agreement with experimental observation. The predicted decrease of island size with increasing oxygen particle density implies also a decrease with increasing oxygen flux. This is also observed. However, the precise relationship between the oxygen flux and the stationary oxygen density cannot be easily derived, because it depends on at least two removal processes, i.e., capture by islands and reevaporation. The latter process must be particularly important for those experiments in which the oxygen fluxes are 5, 10, and 15 times higher than the iron flux. Another complicating factor is the increase in domain size in time due to diffusion processes.

In summary, the exact growth mechanism for  $\text{Fe}_3\text{O}_4$  grown by MBE cannot be determined from these experiments, but it is likely that critical nuclei consist of an iron and an oxygen atom and that Fe diffuses faster than oxygen. Island formation is then dependent on the density of the slower species.

The observed domain sizes and their dependence on growth parameters of course strongly depend on the growth method. These experiments have been performed on  $\text{Fe}_3\text{O}_4$  films grown by MBE where separate iron and oxygen fluxes have been employed. For films grown by sputtering or pulsed laser deposition very different results can be expected. However, for films grown with sputtering similar domain sizes to the ones in our films grown with MBE have been found.<sup>1</sup>

#### IV. CONCLUSIONS

We have grown epitaxial  $\text{Fe}_3\text{O}_4$  films which contain antiphase boundaries (APBs) by MBE and studied the APB density. From the results of the variation in domain size with film thickness and postannealing time, we have shown that the APBs anneal out via a diffusive mechanism, with an activation energy of  $26 \pm 5$  kJ/mol (250 meV). This low activation energy for diffusion of APBs is detrimental for applications such as magnetoresistance devices. Because the APBs structure determines general physical properties such as resistivity and magnetism, it is important to understand the development of the domain structure as a function of growth parameters. A linear relationship has been obtained between the logarithm of the domain size and  $1/T$ . Besides the increase in domain size with growth temperature, we have also studied the influence of the iron and oxygen fluxes. From this data, we propose that critical nuclei are those of  $\text{FeO}$  molecules and that the oxygen species is relatively immobile on the surface and thus determines the domain size.

#### ACKNOWLEDGMENTS

This work was funded by the Netherlands Organization for Scientific Research (NWO). The authors thank John Wheeler for fruitful discussions and H. J. Bruinenberg for technical assistance.



- \*Corresponding author. Email address: w.eerenstein@phys.rug.nl
- <sup>1</sup>D.T. Margulies, F.T. Parker, M.L. Rudee, F.E. Spada, J.N. Chapman, P.R. Aitchison, and A.E. Berkowitz, *Phys. Rev. Lett.* **79**, 5162 (1997).
  - <sup>2</sup>F.C. Voogt, T.T.M. Palstra, L. Niesen, O.C. Rogoianu, M.A. James, and T. Hibma, *Phys. Rev. B* **57**, R8107 (1998).
  - <sup>3</sup>T. Hibma, F.C. Voogt, L. Niesen, P.A.A. van der Heijden, W.J.M. de Jonge, J.J.T.M. Donkers, and P.J. van der Zaag, *J. Appl. Phys.* **85**, 5291 (1999).
  - <sup>4</sup>W. Eerenstein, T.T.M. Palstra, T. Hibma, and S. Celotto, *Phys. Rev. B* **66**, 201101(R) (2002).
  - <sup>5</sup>J.M.D. Coey, A.E. Berkowitz, L.I. Balcells, F.F. Putris, and F.T. Parker, *Appl. Phys. Lett.* **72**, 734 (1998).
  - <sup>6</sup>W. Eerenstein, T.T.M. Palstra, S.S. Saxena, and T. Hibma, *Phys. Rev. Lett.* **88**, 247204 (2002).
  - <sup>7</sup>M. Ziese and H.J. Blythe, *J. Phys.: Condens. Matter* **12**, 13 (2000).
  - <sup>8</sup>A. Yanase and K. Siratori, *J. Phys. Soc. Jpn.* **53**, 312 (1984).
  - <sup>9</sup>S. Kale, S.M. Bhagat, S.E. Lofland, T. Scabarozzi, S.B. Ogale, A. Orozco, S.R. Shinde, T. Venkatesan, B. Hannoyer, B. Mercey, and W. Prellier, *Phys. Rev. B* **64**, 205413 (2001).
  - <sup>10</sup>M.L. Rudee, D.T. Margulies, and A.E. Berkowitz, *Microsc. Microanal.* **3**, 126 (1997).
  - <sup>11</sup>D. Hesse and H. Bethge, *J. Cryst. Growth* **65**, 69 (1983).
  - <sup>12</sup>Andrew Putnis, *Introduction to Minerals Sciences* (Cambridge University, Cambridge, England, 1992), p. 323.
  - <sup>13</sup>A.J. Ardell, N. Mardesich, and C.N.J. Wagner, *Acta Metall.* **27**, 1261 (1979).
  - <sup>14</sup>M.A. Carpenter, *Am. Mineral.* **766**, 1120 (1991).
  - <sup>15</sup>M.A. Carpenter, *Phys. Chem. Miner.* **5**, 119 (1979).
  - <sup>16</sup>R. Dieckmann, *J. Phys. Chem. Solids* **59**, 507 (1998).
  - <sup>17</sup>R. Dieckmann and H. Schmalzried, *Ber. Bunsenges. Phys. Chem.* **81**, 344 (1977).
  - <sup>18</sup>R. Dieckmann and H. Schmalzried, *Ber. Bunsenges. Phys. Chem.* **81**, 414 (1977).
  - <sup>19</sup>R. Dieckmann, *Ber. Bunsenges. Phys. Chem.* **86**, 112 (1982).
  - <sup>20</sup>K.D. Becker, V. von Wurmb, and F.J. Litterst, *J. Phys. Chem. Solids* **54**, 923 (1993).
  - <sup>21</sup>N.L. Peterson, W.K. Chen, and D. Wolf, *J. Phys. Chem. Solids* **41**, 709 (1980).
  - <sup>22</sup>K.D. Becker, V. von Wurmb, and F.J. Litterst, *Hyperfine Interact.* **56**, 1431 (1990).
  - <sup>23</sup>R. Dieckmann, M.R. Hilton, and T.O. Mason, *Ber. Bunsenges. Phys. Chem.* **91**, 59 (1987).
  - <sup>24</sup>A. Atkinson, M.L. O'Dwyer, and R.I. Taylor, *J. Mater. Sci.* **18**, 2371 (1983).
  - <sup>25</sup>D.A. Porter and K.E. Easterling, *Phase Transformations in Metals and Alloys*, 2nd ed. (Chapman and Hall, London, 1992), Chap. 3.
  - <sup>26</sup>J.F. Anderson, M. Kuhn, U. Diebold, K. Shaw, P. Stoyanov, and D. Lind, *Phys. Rev. B* **56**, 9902 (1997).
  - <sup>27</sup>J. Villain, A. Pimpinelli, and D. Wolf, *Comments Condens. Matter Phys.* **16**, 1 (1992).
  - <sup>28</sup>S. Stoyanov and D. Kaschiev, *Current Topics in Materials Science*, edited by E. Kaldis (North-Holland, Amsterdam, 1981).
  - <sup>29</sup>P. Jensen and B. Niemeyer, *Surf. Sci.* **384**, L823 (1997).
  - <sup>30</sup>P. Jensen, H. Larralde, and A. Pimpinelli, *Phys. Rev. B* **55**, 2556 (1997).